Leakage Current Reduction with 240CPWM in Silicon Carbide based Transformerless Grid-connected PV Converter

Hafsa Qamar
School of Electrical, Computer and Energy Engineering
Arizona State University
Tempe, Arizona
hqamar2@asu.edu

Haleema Qamar
School of Electrical, Computer and Energy Engineering
Arizona State University
Tempe, Arizona
hqamar1@asu.edu

Nikhil Korada
School of Electrical, Computer and Energy Engineering
Arizona State University
Tempe, Arizona
nkorada@asu.edu

Madhura Sondharangalla
School of Electrical, Computer and Energy Engineering
Arizona State University
Tempe, Arizona
madhurab@asu.edu

Raja Ayyanar
School of Electrical, Computer and Energy Engineering
Arizona State University
Tempe, Arizona
rayyanar@asu.edu

2022 IEEE Energy Conversion Congress and Exposition (ECCE) | 978-1-7281-9387-8/22/$31.00 ©2022 IEEE | DOI: 10.1109/ECCE50734.2022.9947898

***Abstract*—High leakage current is one of the major reliability concerns in transformerless grid-connected (TLGC) PV converters due to lack of galvanic isolation. Large leakage capacitance of PV modules in TLGC PV systems makes the resonant frequency of the leakage path very low. It forces high leakage current if switching frequency of inverter is close to the resonant frequency as in traditional inverters. Switching frequency can be kept higher than the resonant frequency of the leakage path to achieve lower leakage currents. A relatively new PWM method called 240° clamped PWM (240CPWM) encourages the use of higher switching frequency because of its lowest switching loss. This work deploys 240CPWM in silicon carbide based inverter at switching frequency of 100 kHz that gives 70% saving in leakage current and 4.7 times reduction in AC filter inductor volume as compared to silicon based inverter switching at 10 kHz without compromising the inverter efficiency.**

***Index Terms*—Photovoltaic (PV), Silicon Carbide (SiC) inverter, 240°-Clamped PWM (240CPWM), Common Mode Voltage (CMV), Leakage current**

I. Introduction

Grid-connected photovoltaic (PV) systems have seen exponential growth in the recent years to address environmental hazards from fossil fuels. Transformerless grid-connected (TLGC) PV converters have gained popularity due to low cost and volume. Due to absence of galvanic isolation, leakage current flows through the solar panel parasitic capacitance (C_{PV}) to ground [1]. C_{PV} depends on factors like PV panel, frame structure and weather conditions. C_{PV} is estimated to be 150-200 nF/kWp and it increases from nF to uF range in high power PV systems that becomes the dominating factor for increasing leakage current [2], [3]. High leakage current deteriorates the system performance with severe electromagnetic interference, high total harmonic distortion (THD) and additional losses. Various PWM methods and topological changes are proposed in the literature to address common mode voltage (CMV) and leakage current in TLGC PV converters, for example, reduced CMV PWM (RCMV-PWM) methods reduce CMV and leakage current at the expense of increased switching loss, DC link current stress or THD [2], [4]–[6]. 240° clamped PWM (240CPWM) is a relatively new lowest loss PWM method that does not use any zero state, thereby reducing the CMV and leakage current. 240CPWM was discussed for PV converters in [7]–[12] and for motor drives in [13]–[16] and battery chargers in [17], [18]. Performance evaluation of 240CPMW in TLGC PV converters is carried out in detail in Si based inverter with switching frequency of 10 kHz in [19]. Block diagram of TLGC PV converter under consideration is shown in Fig. 1.

Space vector plane for three phase two level voltage source inverter (VSI) is shown in Fig. 2 (a). Conventional Space Vector PWM (CSVPWM) uses two active states and two zero states (Fig. 2 (b)) while discontinuous PWM method (DPWM1) uses one zero state instead of two (Fig. 2 (c)). With 240CPWM, zero states are completely eliminated and only two nearest active states are used in each sector to synthesize the reference voltage vector (Fig. 2 (d)). Magnitude of peak common mode voltage (CMV) corresponding to zero state and active state is $\pm V_{dc}/2$ and $\pm V_{dc}/6$ respectively. Fig. 3 shows

978-1-7281-9387-8/22/$31.00 ©2022 IEEE

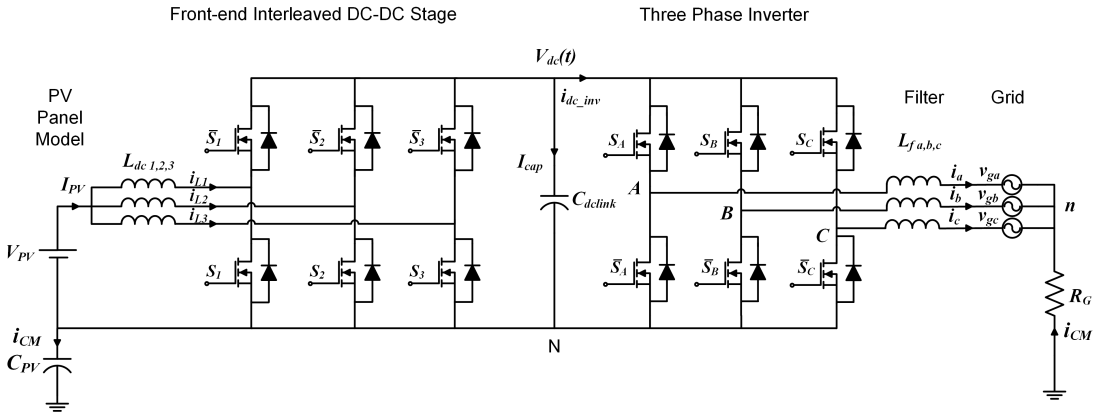

Fig. 1. Block diagram of a two-stage, TLGC PV converter with leakage current path.

CMV waveforms for CSVPWM, DPWM1 and 240CPWM wherein peak CMV for CSVPWM and DPWM1 is $\pm V_{dc}/2$ and peak CMV for 240CPWM is only $\pm V_{dc}/6$ as expected. So, peak CMV for 240CPWM is 66.67% lower than conventional PWM methods because of complete elimination of zero states in 240CPWM.

With 240CPWM, each phase pole is clamped to positive or negative DC rail for 240° in a fundamental cycle as shown in Fig. 4 (b) and (c). Dynamic DC link voltage is required with 240CPWM that becomes part of line-to-line voltages in clamped region (Fig. 4 (d)). 240CPWM requires the cascaded architecture of DC-DC stage followed by DC-AC stage to shape the six-pulse dynamic DC link voltage. 240CPWM can be implemented in most three-phase PV converters since they have DC-DC converter followed by DC-AC inverter in standard configuration. Traditional silicon (Si) based inverters are undergoing a transition with the deployment of wide band gap semiconductor devices like silicon carbide (SiC) due to their superior performance like high efficiency, high switching frequency and high voltage capability. Even with SiC devices, CSVPWM leads to high switching losses at frequencies above 100 kHz. 240CPWM encourages high switching frequency by ensuring lowest switching loss. Fig. 5 shows loss breakdown with switching frequency of 100 kHz at 3 kW using SiC inverter with CSVPWM, DPWM1 and 240CPWM. Switching loss with 240CPWM is reduced by 85% as compared to CSVPWM.

II. CMV and Leakage Current in SiC Inverter

CMV and leakage current analysis with 240CPWM is carried out for motor drive application in [20]. In motor drives, leakage current depends mainly on dv/dt of inverter and partially on CMV because parasitic capacitance of motor is very small (nF range), and it varies significantly from PV application. This work focuses on the CMV and leakage current evaluation with 240CPWM in TLGC PV converter using a high switching frequency SiC inverter. Common mode equivalent circuit of TLGC PV system and its impedance are shown in Fig. 6. Resonant frequency of the leakage path

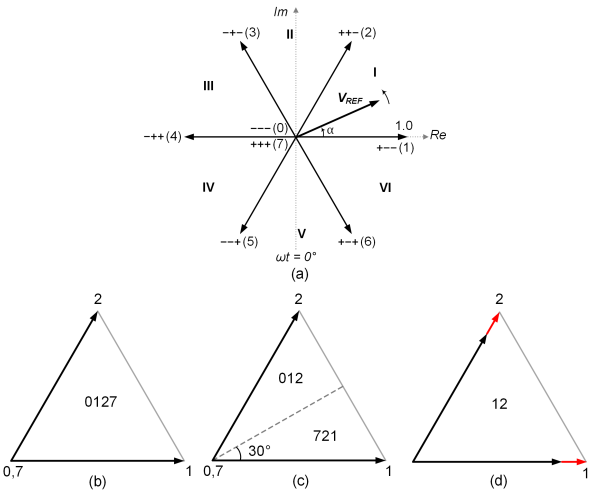

Fig. 2. (a) Space vector plane for three phase two level voltage source inverter, Switching sequence for (b) CSVPWM, (c) DPWM1 and (d) 240CPWM

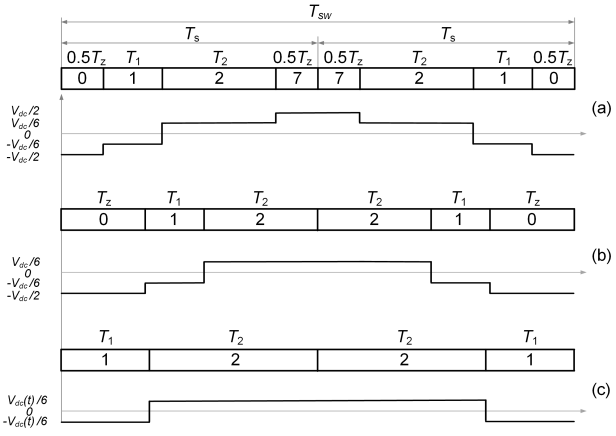

Fig. 3. CMV waveform for (a) CSVPWM, (b) DPWM1 and (c) 240CPWM

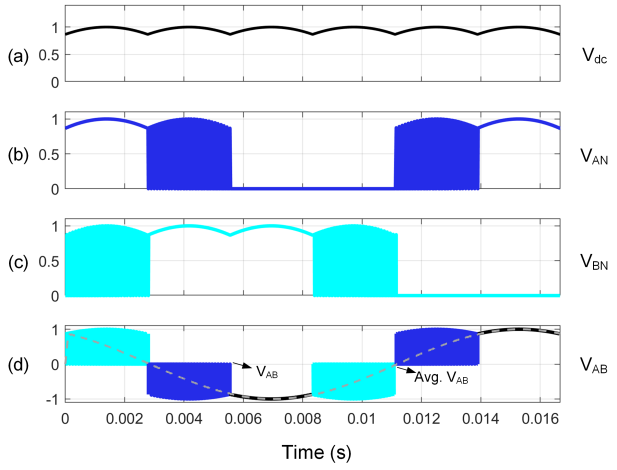

Fig. 4. Voltage waveforms with 240CPWM (a) Dynamic DC link voltage, Switching voltages (b) Phase A, (c) Phase B, (d) Line to line voltage.

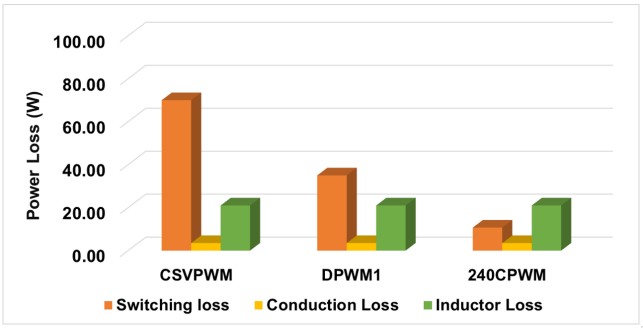

Fig. 5. Loss breakdown using SiC inverter with switching frequency of 100 kHz at 3 kW. Analysis corresponds to DC-AC stage only.

$(f_{r,cm})$ is given by $1/2\pi\sqrt{C_{PV}L_f/3}$ where L_f is the filter inductor. $f_{r,cm}$ is 8 kHz when switching frequency of the inverter $(f_{sw,dcac})$ is 10 kHz (typically in conventional Si IGBTs). $f_{r,cm}$ is very close to the switching frequency and it excites the resonance making leakage current very high. In case of SiC inverters where $f_{sw,dcac}$ is 100 kHz (in our case), $f_{r,cm}$ is 18.4 kHz because of small L_f (Table I) which is very far away from $f_{sw,dcac}$. Common mode equivalent circuit offers high impedance that reduces the leakage current significantly as compared to Si IGBT inverter.

PLECS simulation results of 240CPWM with Si IGBT inverter and SiC inverter with $f_{sw,dcac}$ of 10 kHz and 100 kHz are shown in Fig. 7 and Fig. 8 respectively both with CSVPWM and DPWM1. CMV and leakage current with CSVPWM and DPWM1 are very high in Si inverter as expected. With SiC inverter ($f_{sw,dcac}$=100 kHz), leakage current is reduced substantially because the switching frequency is very far away from resonant frequency of the leakage path. PLECS simulation results for 240CPWM with $f_{sw,dcac}$ of 10 kHz and 100 kHz are shown in Fig. 9 (a) and (b) respectively. RMS CMV ($V_{CM,RMS}$) remains the same but RMS leakage current ($I_{CM,RMS}$) is reduced by 70% for

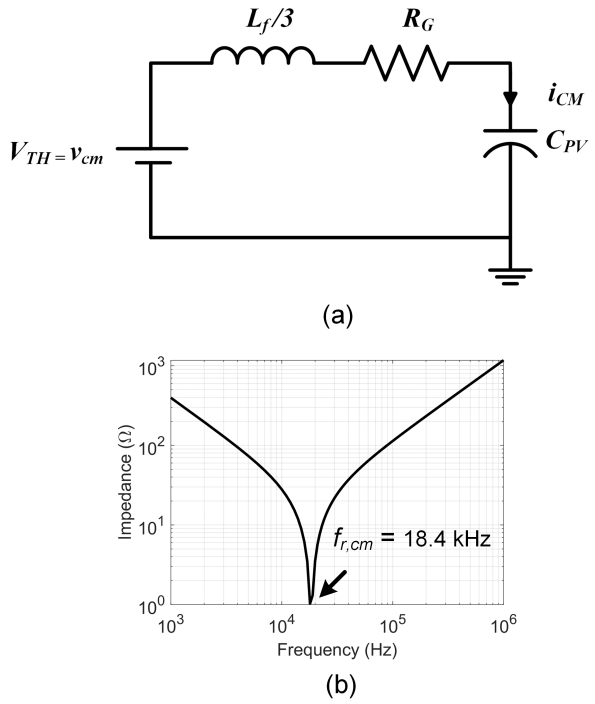

Fig. 6. Common mode equivalent circuit, (b) Impedance of common mode equivalent circuit in TLGC PV converter.

SiC inverter ($f_{sw,dcac}$=100 kHz) as compared to Si inverter ($f_{sw,dcac}$=10 kHz) with 240CPWM.

III. Experimental Validation

The experimental set-up is tested at 1 kW and its specifications are shown in Table I. Table 2 gives the details of gate driver, Si IGBT and SiC MOSFETS. The experimental set-up consists of a DC-DC converter which is a three phase interleaved boost converter and a three phase DC-AC inverter, both with SiC MOSFETs. The picture of experimental set-up is shown in Fig. 10. Inductor design for SiC inverter shows that inductor volume for SiC inverter is 245 cm^3 that is 4.7 times lower than inductor volume for Si inverter (1170 cm^3) as shown in Fig. 11.

The performance of 240CPWM in terms of CMV and leakage current is compared for low and high switching frequency inverter. For low switching frequency, Si IGBT based inverter switching at 10 kHz is selected. Silicon Carbide inverter switching at 100 kHz is designed to validate the common mode performance of 240CPWM in high switching frequency inverters. The required waveforms are captured by a LeCroy HDO8038 oscilloscope with 10 MHz sampling frequency using LeCroy CP030 30 A 50 MHz current probes and LeCroy ADP305 100 MHz 1400 V differential voltage probes.

The experimental results in grid connected mode with 240CPWM at 1 kW and 170 V line to line RMS voltage with leakage path are shown in Fig. 12 and Fig. 13. Fig. 12 shows the CMV and leakage current in Si IGBT based inverter with

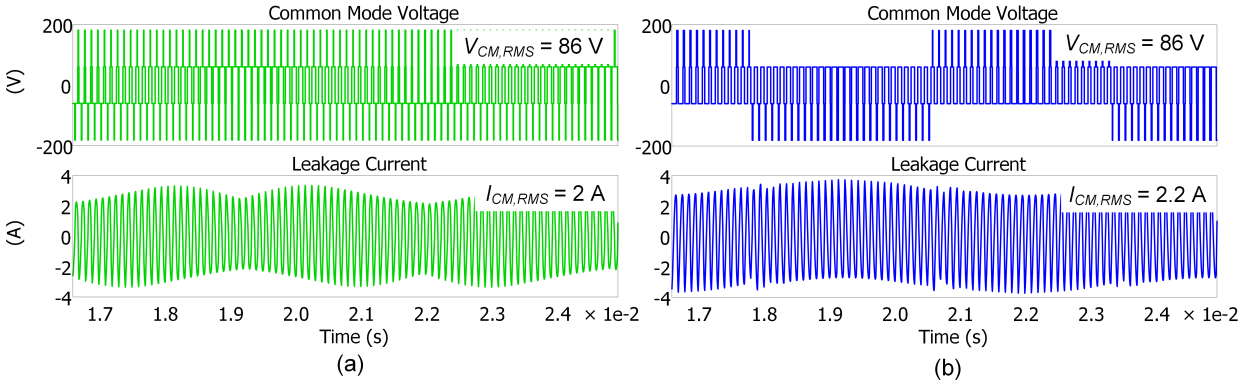

Fig. 7. CMV and Leakage current for Si inverter with switching frequency of 10 kHz at 3 kW (a) CSVPWM and (b) DPWM1

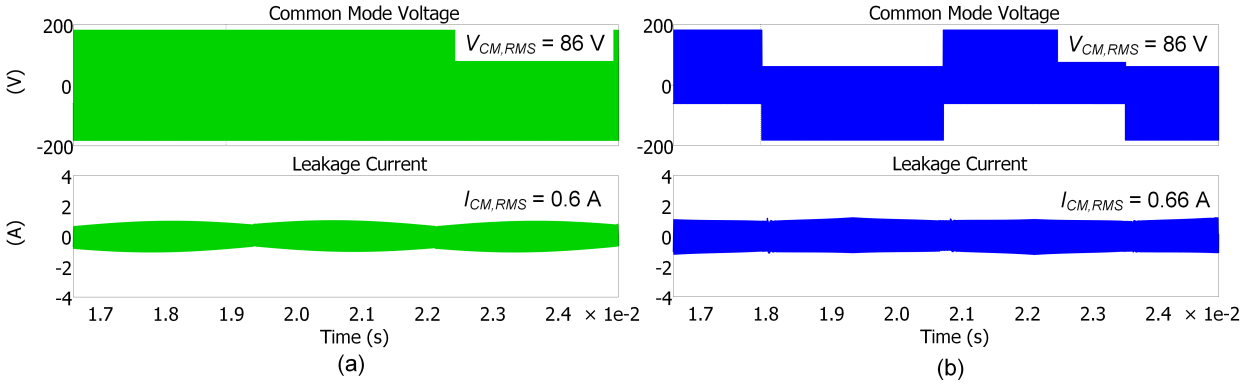

Fig. 8. CMV and Leakage current for SiC inverter with switching frequency of 100 kHz at 3 kW (a) CSVPWM and (b) DPWM1

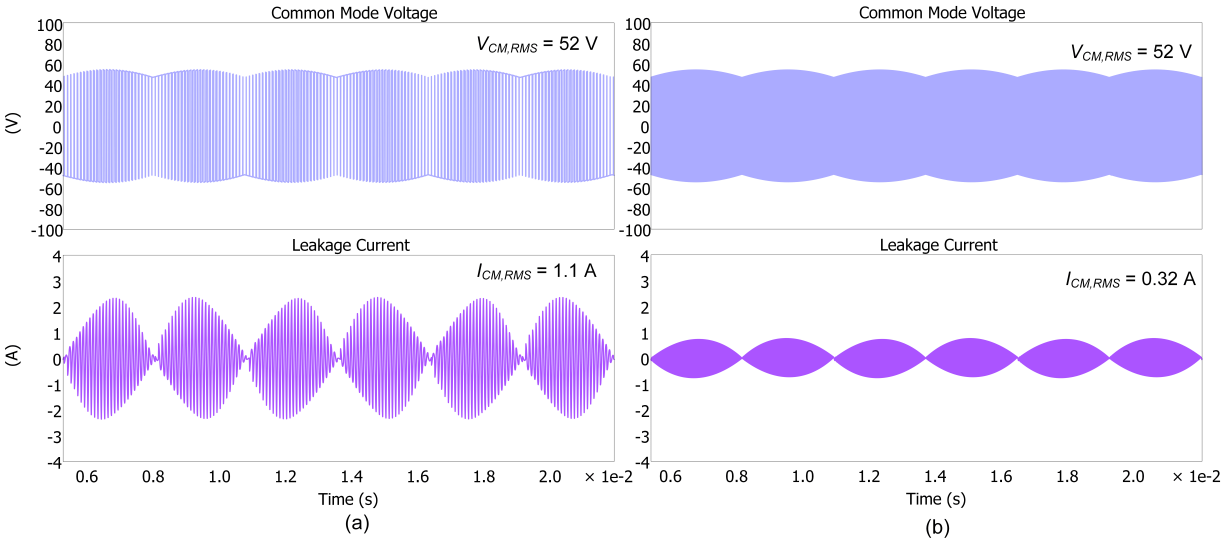

Fig. 9. CMV and leakage current for 240CPWM at 3 kW (a) Si inverter, $f_{sw,dcac}$ = 10 kHz (b) SiC inverter, $f_{sw,dcac}$ = 100 kHz

TABLE I
SPECIFICATIONS OF PLECS SIMULATION AND EXPERIMENTAL SETUP.

	Parameter	Value
DC-DC Stage	Input voltage V_{PV}	120 V
	DC link Voltage peak for 240CPWM $V_{dc,pk}$	240 V
	Number of interleaved phases n	3
	Inductance L_{dc}	560 uH
	DC link Capacitance C_{dc}	20 uF
	Switching frequency $f_{sw,dcdc}$	50 kHz
DC-AC Stage	Output Power P	1 kW
	Grid voltage v_g (line-to-line RMS)	170 V
	Filter Inductance L_f	560 uH
	Switching frequency $f_{sw,dcac}$	100 kHz
	Grid frequency f_1	60 Hz
Leakage Path	Resistance R_G	10 Ω
	Capacitance C_{PV}	0.4 uF

TABLE II
SPECIFICATIONS OF SWITCHES AND GATE DRIVER

Component	Parameter	Value
Gate Driver	Part number	CGD15SG00D2
SiC MOSFET	Part number	C3M0016120K
	On resistance $R_{ds,on}$	16 mΩ
	Voltage rating	1200 V
Si IGBT	Part number	FF200R12KE4

switching frequency of 10 kHz whereas Fig. 13 is with SiC inverter with switching frequency of 100 kHz. It can be seen that the CMV remains similar irrespective of the switching frequency of inverter but leakage current is greatly reduced at 100 kHz as compared to 10 kHz.

The zoomed in experimental waveforms corresponding to Fig. 12 and Fig. 13 are shown in Fig. 14. RMS CMV $V_{CM,RMS}$ = 35.9 V for $f_{sw,dcac}$ = 10 kHz and it is 35 V for $f_{sw,dcac}$ = 100 kHz. RMS leakage current is reduced from 720 mA at 10 kHz to just 217 mA at 100 kHz. Hence, RMS CMV remains similar for both the cases but RMS leakage current is reduced by 70% at 100 kHz as compared to the RMS leakage current at 10 kHz.

IV. CONCLUSION AND FUTURE WORK

High leakage current raises safety concerns in TLCG PV converters due to high leakage capacitance in the leakage path. Traditionally, switching frequency of PV inverters is low which is close to the resonant frequency of leakage path that forces high leakage current. Switching frequency of inverter can be shifted away from resonant frequency of leakage path by increasing the switching frequency of inverter. 240CPWM is the lowest switching loss PWM method that allows high switching frequency without compromising efficiency in inverter, thereby, minimizing the leakage current. The experimental results of CMV and leakage current with Si inverter and SiC inverter at 1 kW are presented with 240CPWM. With SiC inverter switching at 100 kHz, 70%

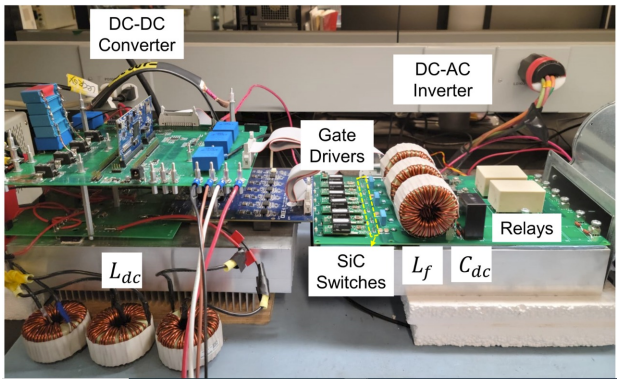

Fig. 10. Picture of experimental set-up.

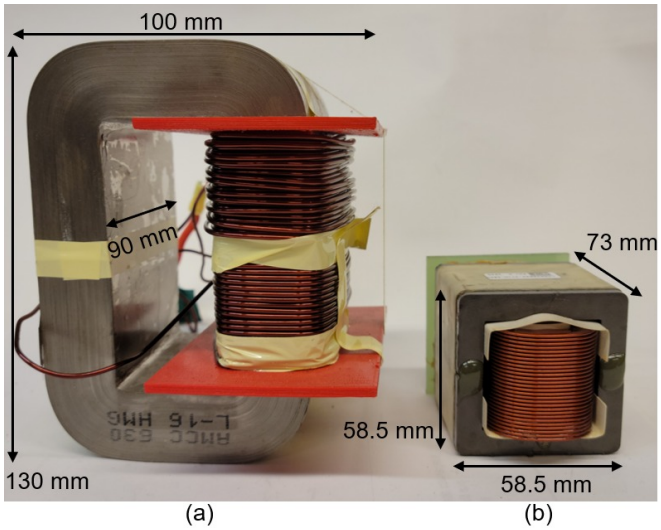

Fig. 11. Inductor for (a) Si inverter, (b) SiC inverter.

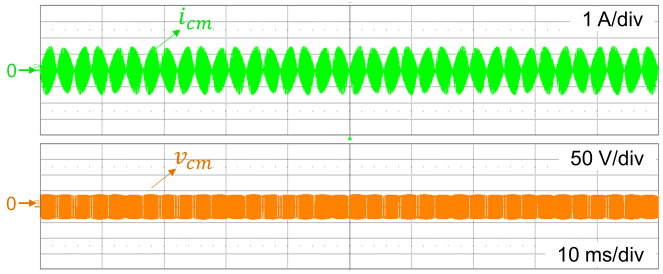

Fig. 12. CMV (50 V/div) and leakage current (1 A/div) at 1 kW in grid-connected mode at switching frequency of 10 kHz (time scale = 10 ms/div).

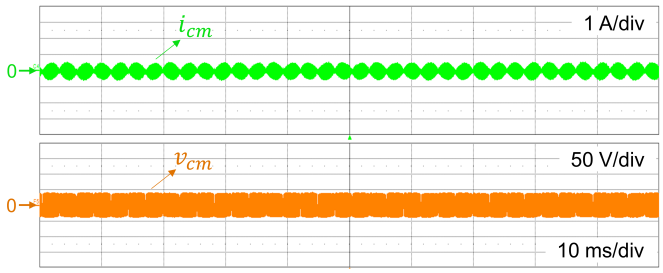

Fig. 13. CMV (50 V/div) and leakage current (1 A/div) at 1 kW in grid-connected mode at switching frequency of 100 kHz (time scale = 10 ms/div).

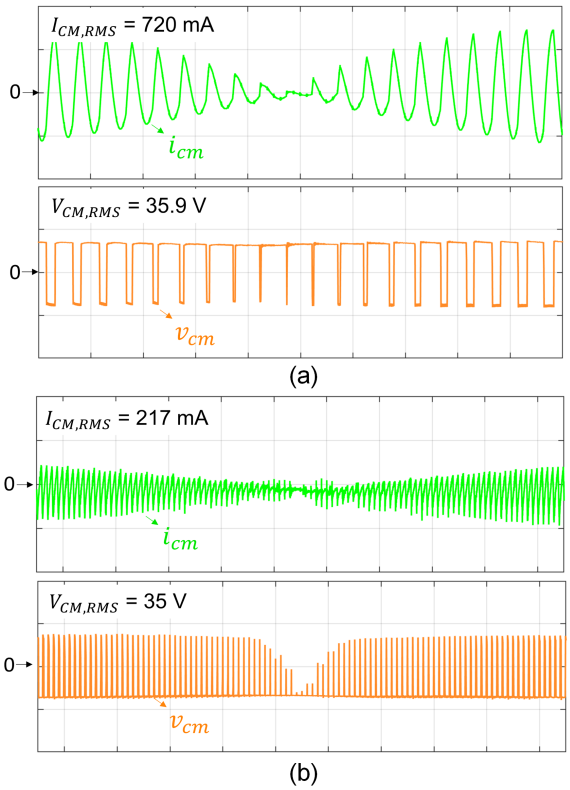

Fig. 14. CMV (50 V/div) and leakage current (1 A/div) at 1 kW in grid-connected mode at switching frequency of (a) 10 kHz (b) 100 kHz (time scale = 200 us/div).

saving in leakage current and 4.7 times reduction in AC filter inductor are achieved without compromising the inverter efficiency as compared to Si inverter switching at 10 kHz with 240CPWM.

ACKNOWLEDGMENT

This work made use of facility supported by the National Science Foundation Industry-University Collaborative Research Center for Efficient Vehicles and Sustainable Transportation Systems under Award No. IIP-1624842.

REFERENCES

[1] H. Xiao, "Overview of Transformerless Photovoltaic Grid-Connected Inverters," in IEEE Transactions on Power Electronics, vol. 36, no. 1, pp. 533-548, Jan. 2021, doi: 10.1109/TPEL.2020.3003721.

[2] C. -C. Hou, C. -C. Shih, P. -T. Cheng and A. M. Hava, "Common-Mode Voltage Reduction Pulsewidth Modulation Techniques for Three-Phase Grid-Connected Converters," in IEEE Transactions on Power Electronics, vol. 28, no. 4, pp. 1971-1979, April 2013, doi: 10.1109/TPEL.2012.2196712.

[3] J. Roy, Y. Xia and R. Ayyanar, "Performance evaluation of single-phase transfomer-less PV inverter topologies," 2018 IEEE Applied Power Electronics Conference and Exposition (APEC), 2018, pp. 3250-3255, doi: 10.1109/APEC.2018.8341568.

[4] J. Xu, J. Han, Y. Wang, S. Habib and H. Tang, "A Novel Scalar PWM Method to Reduce Leakage Current in Three-Phase Two-Level Transformerless Grid-Connected VSIs," in IEEE Transactions on Industrial Electronics, vol. 67, no. 5, pp. 3788-3797, May 2020, doi: 10.1109/TIE.2019.2920597.

[5] J. Xu, J. Han, Y. Wang, M. Ali and H. Tang, "High-Frequency SiC Three-Phase VSIs With Common-Mode Voltage Reduction and Improved Performance Using Novel Tri-State PWM Method," in IEEE Transactions on Power Electronics, vol. 34, no. 2, pp. 1809-1822, Feb. 2019, doi: 10.1109/TPEL.2018.2829530.

[6] E. Un and A. M. Hava, "A Near-State PWM Method With Reduced Switching Losses and Reduced Common-Mode Voltage for Three-Phase Voltage Source Inverters," in IEEE Transactions on Industry Applications, vol. 45, no. 2, pp. 782-793, March-april 2009, doi: 10.1109/TIA.2009.2013580.

[7] K. Rigbers, S. Schroder, R. W. de Doncker, P. Lurkens, M. Wendt and U. Boke, "High-efficient Soft-Switching Converter for Three-Phase Grid Connections of Renewable Energy Systems," 2005 International Conference on Power Electronics and Drives Systems, 2005, pp. 246-250, doi: 10.1109/PEDS.2005.1619693.

[8] J. Shen, K. Rigbers, C. P. Dick and R. W. De Doncker, "A Dynamic Boost Converter Input Stage for a Double 120° Flattop Modulation Based Three-Phase Inverter," 2008 IEEE Industry Applications Society Annual Meeting, 2008, pp. 1-7, doi: 10.1109/08IAS.2008.311.

[9] S. Engel, K. Rigbers, and R. W. De Doncker, "Digital repetitive control of a three-phase flat-top-modulated grid tie solar inverter," in 2009 13th European Conference on Power Electronics and Applications, 2009, pp. 1–10.

[10] H. Fujita, "A three-phase voltage-source solar power conditioner using a single-phase PWM control method," 2009 IEEE Energy Conversion Congress and Exposition, 2009, pp. 3748-3754, doi: 10.1109/ECCE.2009.5316305.

[11] H. Fujita, "Switching loss analysis of a three-phase solar power conditioner using a single-phase PWM control method," 2010 IEEE Energy Conversion Congress and Exposition, 2010, pp. 618-623, doi: 10.1109/ECCE.2010.5617954.

[12] H. Qamar, H. Qamar, N. Korada and R. Ayyanar, "240°-Clamped PWM Applied to Transformerless Grid Connected PV Converters With Reduced Common Mode Voltage and Superior Performance Metrics," in IEEE Open Journal of Power Electronics, vol. 3, pp. 153-167, 2022, doi: 10.1109/OJPEL.2022.3155053.

[13] Q. Lei and F. Z. Peng, "Space vector pulsewidth amplitude modulation for a buck–boost voltage/current source inverter," IEEE Trans. power Electron., vol. 29, no. 1, pp. 266–274, 2013.

[14] D. Wu, H. Qamar, H. Qamar, and R. Ayyanar, "Comprehensive Analysis and Experimental Validation of a New 240°-Clamped Space Vector PWM Technique Eliminating Zero States for EV Traction Inverters with Dynamic DC Link," IEEE Trans. Power Electron., vol. 35, no. 12, pp. 13295–13307, 2020.

[15] H. Qamar, H. Qamar, D. Wu, and R. Ayyanar, "DC Link Capacitor Sizing for 240°-Clamped Space Vector PWM for EV Traction Inverters," in IEEE Applied Power Electronics Conference and Exposition-APEC 2021., 2021.

[16] M. Antivachis, J. A. Anderson, D. Bortis and J. W. Kolar, "Analysis of a synergetically controlled two-stage three-phase DC/AC buck-boost converter," in CPSS Transactions on Power Electronics and Applications, vol. 5, no. 1, pp. 34-53, March 2020, doi: 10.24295/CPSSTPEA.2020.00004.

[17] J. A. Anderson, M. Haider, D. Bortis, J. W. Kolar, M. Kasper, and G. Deboy, "New Synergetic Control of a 20kW Isolated VIENNA Rectifier Front-End EV Battery Charger," in 2019 20th Workshop on Control and Modeling for Power Electronics (COMPEL), 2019, pp. 1–8.

[18] D. Menzi, D. Bortis and J. W. Kolar, "Three-Phase Two-Phase-Clamped Boost-Buck Unity Power Factor Rectifier Employing Novel Variable DC Link Voltage Input Current Control," 2018 IEEE International Power Electronics and Application Conference and Exposition (PEAC), 2018, pp. 1-8, doi: 10.1109/PEAC.2018.8590599.

[19] H. Qamar, H. Qamar, N. Korada and R. Ayyanar, "240°-Clamped PWM Applied to Transformerless Grid Connected PV Converters With Reduced Common Mode Voltage and Superior Performance Metrics," in IEEE Open Journal of Power Electronics, vol. 3, pp. 153-167, 2022, doi: 10.1109/OJPEL.2022.3155053.

[20] H. Qamar, H. Qamar and R. Ayyanar, "Performance Analysis and Experimental Validation of 240°-Clamped Space Vector PWM to Minimize Common Mode Voltage and Leakage Current in EV/HEV Traction Drives," in IEEE Transactions on Transportation Electrification, vol. 8, no. 1, pp. 196-208, March 2022, doi: 10.1109/TTE.2021.3108957.